Dendritic instability of the magnetic flux in thermally anisotropic type-II superconductors

E. E. Dvash, I. Shapiro, and B. Ya. Shapiro
Department of Physics, Institute of Superconductivity, Bar-Ilan University, Ramat-Gan 52900, Israel
(Received 18 January 2009; revised manuscript received 30 August 2009; published 27 October 2009)

The thermomagnetic instability of the Bean critical state in a layered type-II superconducting slab subjected to an external magnetic field increasing with constant rate is studied theoretically. It is shown that the strong anisotropy of thermal conductivity significantly affects the instability onset. By applying a linear analysis of Maxwell and thermal diffusion equations, the criteria for the nonuniform instability, the characteristic size of the flux pattern, and the stability-instability coexistence line were obtained.

DOI: 10.1103/PhysRevB.80.134522 PACS number(s): 74.20.De, 74.25.Qt, 74.25.Ha

I. INTRODUCTION

The dynamics of magnetic flux front, penetrating type II superconductors and its instability has been studied by a variety of techniques, (see Ref. 1 and references therein). In many experimental situations, when the superconducting sample in the Bean critical state is subjected to a slowly increasing external magnetic field $H_{ext}=B_{ext}/\mu_0$, often a flat magnetic front demonstrates its instability. The unstable flux pattern emerges when the ramp rate of the external magnetic induction $\dot{B}_{ext}$ exceeds some critical value $\dot{B}_c$, otherwise the instability develops uniformly if the external magnetic field exceeds some critical value B_a (Ref. 2) (see (Fig. 1).[3]

The thermomagnetic instability occurs due to local perturbations of the vortex matter and by the heat released by the vortex dynamics resulting in additional heating of the vortex matter. This positive feedback process leading to the thermal softening of the vortex matter is responsible for the instability. Usually, the instability develops around a well-defined flat flux profile of the Bean critical state. The conventional theory for thermomagnetic instability predicts "uniform" flux jumps, when the unstable flux front is essentially flat. This prediction holds for many experimental conditions, but not for all. In particular, magneto-optical techniques have revealed a broad class of spatial magnetic-flux instabilities, including magnetic macroturbulence,[4] finger pattern instability,[5,6] and dendritic instability.[7] The spatially nonuniform instabilities of the magnetic flux in films are observed both in slightly anisotropic high-temperature superconducting materials[5] and in isotropic conventional superconductors such as Nb.[7]

Thermomagnetic instability in an isotropic type-II superconducting slab and in a thin film was considered theoretically in Refs. 1, 3, and 8–11. These studies predicted that nonlocality of the Maxwell equations for a superconducting geometry is essential for the establishment of a nonuniform flux distribution, while in an isotropic superconducting slab, where the Maxwell equations are local, the nonuniform instability arises only under a high rate of the increasing external magnetic field, which is difficult to reach in experiments.[3]

It seems that the nonuniform flux instability in strongly anisotropic superconductors is rather similar to those observed in superconducting films rather than in isotropic slabs. Despite the role of the anisotropy in pattern creation, it has been considered in some simple models (see Refs. 12 and 15), *and there is possibly still no general theory of this phenomenon.*

In strongly anisotropic layered superconductors both the vortex viscosity[12] and the thermal conductivity[13] are described by the tensors ($\eta_{\alpha\beta}, \kappa_{\alpha\beta}$ correspondingly) with highly different in-plane and across-the-plane directions of the main tensor's components.[14,15] On the other hand, as the anisotropy of the vortex viscosity is in the focus of investigations,[12,15] the anisotropy of the thermal conductivity is usually ignored, while this anisotropy is a well-pronounced property of many layered systems including high-temperature superconductors.[13]

The thermal conductivity used plays an important role in the onset of the flux pattern creation.[3] In fact, the spatially nonuniform thermomagnetic instability appears when the thermal diffusion is slower than the diffusion of the vortices. In particular, an effective decrease in the effective ratio $\tau = t_M/t_h$ (here t_M, t_h are the magnetic and thermal diffusion times, respectively) is responsible for nonuniform, dendritic instability of magnetic flux in thin films.[1,10] In this paper, we show that the anisotropy of the thermal conductivity in a bulk sample plays an essential role assisting in the creation of the nonuniform thermomagnetic instability.

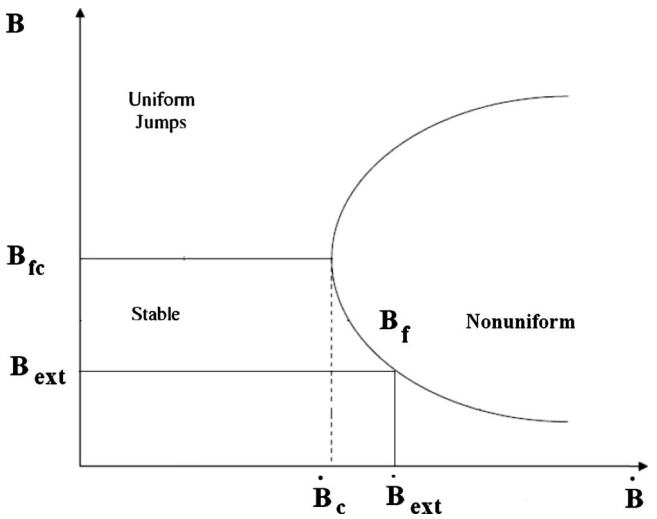

FIG. 1. Phase diagram of the instability in the B-$\dot{B}$ plane. Here B_{ext} is the external magnetic induction, $\dot{B}_c$ is the critical induction required for the development of the nonuniform instability, and B_{fc} is the border between uniform and fingering instabilities.

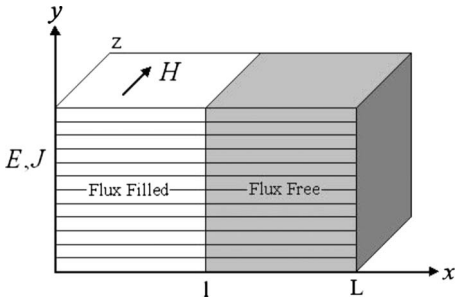

FIG. 2. Geometry of the problem. Here l is the Bean penetration length and L is the thickness of the slab.

II. MODEL AND BASIC EQUATIONS

We will study the instability in geometry, where an anisotropic layered superconducting slab fills the space $0<x<L$, $-\infty<y<\infty$ (Fig. 2) the external, slowly increasing magnetic field H is parallel to the z axis, so that the screening current J flows along the y axis. The a-b plane of the layered structure is placed in the x-z plane, where the c axis is parallel to the y direction, and $l \ll L$ is the penetration length of the magnetic induction. The ramping rate of the external magnetic field is assumed to be constant. The slab is placed in a coolant with temperature T_0.

We assume that the magnetic flux penetrates the slab through one edge (y-z plane). The current, the magnetic field, and the electric-field distributions in the sample are determined by the Maxwell equations

$$-\frac{\partial \mathbf{B}}{\partial t} = \nabla \times \mathbf{E}, \quad \nabla \times \mathbf{B} = \mu_0 \mathbf{J}, \tag{1}$$

with the appropriate boundary conditions

$$\mathbf{B}|_{x=0} = \mu_0 \mathbf{H}; \quad \left.\frac{\partial \mathbf{H}}{\partial t}\right|_{x=0} = const. \tag{2}$$

(We assume that the local magnetic induction in the flux-penetrated part of the slab is greater than the first critical field and $\mathbf{B}=[0,0,\mathbf{B}_z(x,y)]$). The flux flow resistivity is caused by the vortex motion. In the anisotropic case

$$\eta_{xx} v_x = \mathbf{J}_y \times \boldsymbol{\varphi}_0; \quad \eta_{yy} v_y = \mathbf{J}_x \times \boldsymbol{\varphi}_0, \tag{3}$$

where η_{xx}, η_{yy} are the main viscosity tensor components of the vortices in the x and y (in-planes and across-the-planes) directions, respectively, and φ_0 is the flux of a single vortex. This motion creates a voltage $\mathbf{E}=\boldsymbol{\varphi}_0 \times \mathbf{v}$, and, therefore, the current-voltage characteristic will be

$$\mathbf{J}_x = \frac{\eta_{yy}}{\varphi_0^2}\frac{\mathbf{E}_x}{E}, \quad \mathbf{J}_y = \frac{\eta_{xx}}{\varphi_0^2}\frac{\mathbf{E}_y}{E}. \tag{4}$$

Therefore, the electric anisotropy parameter can be written by

$$\gamma = \frac{\eta_{yy}}{\eta_{xx}}. \tag{5}$$

In this case, the voltage-current characteristics are also anisotropic and can be represented in the form

$$\mathbf{J}_x = \gamma J(T,B,\mathbf{E})\frac{\mathbf{E}_x}{E}, \quad \mathbf{J}_y = J(T,B,\mathbf{E})\frac{\mathbf{E}_y}{E}, \tag{6}$$

where $J(T,B,\mathbf{E})$ dependence is strongly nonlinear and describes the in-plane current transport, and γ is the parameter of the electric anisotropy. The set of the Maxwell equations must be completed by the corresponding anisotropic thermal-conductivity equation

$$C\frac{\partial T}{\partial t} = \kappa_\perp \nabla_y^2 T + \kappa_\parallel \nabla_x^2 T + \mathbf{J}\cdot\mathbf{E} \tag{7}$$

with the Newton cooling law[1] as the boundary conditions at both sides of the slab (see Fig. 2)

$$\left.\frac{\partial T}{\partial x}\right|_{x=0,L} = \pm h_0 (T - T_0)|_{x=0,L}, \tag{8}$$

where T_0 and h_0 are the effective environment temperature and heat transfer constant, respectively. Here C is the specific heat, $\kappa_\perp, \kappa_\parallel$ are the thermal diffusion coefficients. In our case, the thermal-conductivity anisotropy parameter

$$\epsilon = \frac{\kappa_\perp}{\kappa_\parallel}, \tag{9}$$

is smaller when the thermal anisotropy is stronger. (These equations are valid only if x and y coincide with the symmetry axis of the crystalline lattice).

Considering the Bean critical state $[J(T,B,\mathbf{E})=J_c(T,\mathbf{E})]$, where the critical current density J_c describes the current transport perpendicular to the layers as an initial state from which the instability evolves, one obtains from the Eqs. (1)–(7)

$$\mathbf{E} = (0, E_{0y}); E_{0y} = (\mu_0 \partial H/\partial t)(l - x). \tag{10}$$

Here l is the Bean penetration length in the x direction (see Fig. 2). The solution of the Eqs. (7) and (8) completed by the continuity conditions for the temperature and its derivative at the Bean front $(x=l)$ reads $(L \gg l)$

$$T = T_0 + \frac{\mu_0 J_c \dot{H}}{6\kappa_\parallel}\begin{cases} \left[x^3 - 3lx^2 + l^2\left(\frac{3+3Lh_0-lh_0}{2+Lh_0}\right)x + \frac{l^2}{h_0}\left(\frac{3+3Lh_0-lh_0}{2+Lh_0}\right)\right] & x<l \\ -l^2\left(\frac{lh_0+3}{2+Lh_0}\right)x + l^2\left(\frac{lh_0+3}{2+Lh_0}\right)\left(\frac{1}{h_0}+L\right) & l<x<L \end{cases}. \tag{11}$$

From the symmetry of the problem $E_x=0$. Restricting ourselves by the condition $h_0 L \ll 1$ (a nearly thermally insulated surface), one obtains the background temperature $T \simeq T_0$ to the leading order in

$$\frac{l^2}{4T_0}\frac{\mu_0 J_c \dot{H}}{\kappa_\parallel h_0} \ll 1. \tag{12}$$

The background electric field can be replaced by its average over the Bean layer value

$$E_{0y} = \mu_0 \frac{l}{2}\frac{\partial H}{\partial t} = const. \tag{13}$$

This assumption is correct when the wavelength of the instability in the x direction is smaller than the Bean penetration length $\lambda_x < l$ [Wentzel-Kramers-Brillouin (WKB) approximation[2,3]].

The exact form of the current-voltage curve is not crucially important. The only important point is that the E-J curve is very steep, and anisotropic, and its logarithmic derivative is large

$$n(E) = (\partial \ln E/\partial \ln J) \simeq J_c/\sigma_y E \gg 1, \tag{14}$$

where $\sigma_y = (\partial J/\partial E)_{J=J_c}$ is the differential conductivity. At low electric fields, the $E(J)$ curve is often approximated by a power law $E \propto J^n$, where $n \gg 1$ is large and is assumed independent of the electric field. (In the flux flow regime $\sigma(E) = \sigma_{BS}$ is the Bardeen-Stephen flux flow Ohmic conductivity and $n(E) = J_c/\sigma_{BS}E$, however, we restrict ourselves to the case of low electric field).

III. LINEAR STABILITY ANALYSIS

It is widely accepted that linear stability analysis is an essentially robust method of studying dynamic systems.[16] In our case, the linearization of Eqs. (1)–(7) under small perturbation of temperature and the electric field reads

$$T = T_0 + \delta T(x,y,t), \quad \mathbf{E} = E_{0y} + \delta \mathbf{E}_\alpha(x,y,t), \quad \alpha = x,y. \tag{15}$$

These fluctuations immediately result in small perturbations of the current density

$$\delta \mathbf{J}_x = \gamma J(T,E_x)\frac{\delta \mathbf{E}_x}{E}, \quad \delta \mathbf{J}_y = \frac{\partial J}{\partial T}\delta T + \sigma_y \delta E_y. \tag{16}$$

The perturbed heat diffusion equation in this case has the form

$$C\frac{\partial \delta T}{\partial t} = \kappa_\perp \nabla_y^2 \delta T + \kappa_\parallel \nabla_x^2 \delta T + \mathbf{E}_y \delta \mathbf{J}_y + \mathbf{J}_y \delta \mathbf{E}_y. \tag{17}$$

These equations must be supplemented by the boundary conditions for fluctuations at the sample surfaces $(x=0,L)$ and at the flux front $(x=l)$ (see Fig. 2). Since the magnetic field at the slab surface is equal to the applied field, the perturbation at the surface is zero, $\delta H_z = 0$ and the first boundary condition reads

$$\left(\frac{\partial \delta E_y}{\partial x}\right)_{x=0} = 0. \tag{18}$$

This condition also means that the current does not flow across the sample surface, $\delta J_x \propto \delta E_x = 0$ at $x=0$. In the flux-free region, $x > l$, the electric field decays on the scale of the London penetration depth, which is much smaller than any spatial scale of the problem. Therefore, the continuity of the tangential component of the electric field requires

$$\delta E_y(x=l) = 0, \tag{19}$$

which are satisfied for $\delta E_y \propto \cos(K_x x)$ with $K_x = \pi/2l$. Estimating the maximal length of the temperature fluctuation in the x direction as l, one obtains for sufficiently small h_0 $[h_0\lambda_x < 1, \lambda_x < l$ see Eq. (12)]

$$\left(\frac{\partial \delta T}{\partial x}\right)_{x=0} = h_0 \delta T|_{x=0} \to 0, \tag{20}$$

from the boundary condition [Eq. (8)]. It allows one to look for a solution of the Eq. (17) in the form

$$\delta T = T^* \theta \cos(k_x \xi)\exp(\lambda t/t_0 + i k_y \eta), \tag{21}$$

where

$$T^* = \left[\frac{1}{J}\frac{\partial J}{\partial T}\right]^{-1}_{J=J_c, \mathbf{E}=E} \tag{22}$$

and

$$\delta \mathbf{E}_x = E\varepsilon_x \sin(k_x \xi)\exp(\lambda t/t_0 + i k_y \eta), \tag{23}$$

$$\delta \mathbf{E}_y = E\varepsilon_y \cos(k_x \xi)\exp(\lambda t/t_0 + i k_y \eta), \tag{24}$$

where $k_{x,y}$ are the dimensionless wave vectors and

$$\eta = y/w; \quad \xi = x/w; \tag{25}$$

$$t_0 = \frac{\sigma_y C T^*}{J_c^2} = \mu_0 \sigma_y w^2; \quad w^2 = \frac{C T^*}{\mu_0 J_c^2}. \tag{26}$$

Using the Maxwell relation for fluctuations

$$\nabla \times \nabla \times \delta \mathbf{E} = -\mu_0 \frac{\partial \delta \mathbf{J}}{\partial t} \tag{27}$$

one obtains the set of equations

$$(\lambda \gamma n + k_y^2)\varepsilon_x - i k_x k_y \varepsilon_y = 0, \tag{28}$$

$$-i k_x k_y \varepsilon_x - (k_x^2 + \lambda)\varepsilon_y + \lambda n \theta = 0, \tag{29}$$

$$(1 + 1/n)\varepsilon_y - \left[\lambda n + \tau n\left(k_y^2 + \frac{1}{\epsilon}k_x^2\right) + 1\right]\theta = 0, \tag{30}$$

where

$$\tau = t_M/t_h = \mu_0 \sigma_y \kappa_\perp / C = \epsilon \tau_I. \tag{31}$$

Here $\tau_I = \mu_0 \sigma_y \kappa_\parallel / C$ is the thermal parameter for an isotropic slab. This set of equations has a nontrivial solution when the rate growth λ obeys the equation

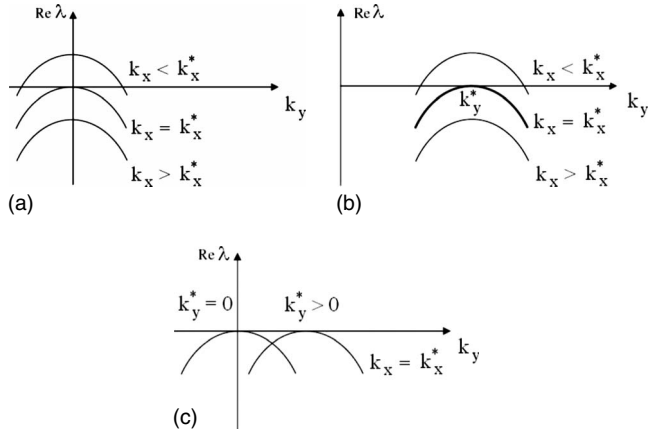

FIG. 3. (a) Uniform instability criterion. (b) Nonuniform instability criterion. (c) Uniform-nonuniform instability border.

$$\lambda^2 + P\lambda + S = 0, \tag{32}$$

and

$$P = k_x^2 + \frac{k_y^2}{\gamma n} + \tau\left(k_y^2 + \frac{1}{\epsilon}k_x^2\right) - 1, \tag{33}$$

$$S = \frac{\tau\left(k_y^2 + \frac{1}{\epsilon}k_x^2\right)(k_x^2\gamma n + k_y^2) + k_x^2\gamma - k_y^2}{\gamma n}. \tag{34}$$

(Note that setting $\gamma, \epsilon = 1$ in the Eqs. (32)–(34) we obtain the dispersion relation from Ref. 3 for isotropic superconductors).

The instability appears when $\mathrm{Re}\,\lambda(k_x, k_y, \epsilon, n, \gamma) > 0$. Depending on the parameters of the anisotropy of the system, one can separate the shape of the unstable front under two scenarios: (1) uniform, when the maximum value of the rate grow function Re λ has a contact point at $k_y = 0$ and (2) nonuniform, with the touching point at $k_y \neq 0$. This scenario attracts special interest because it is used responsible for dendritic and fingering instabilities [see Figs. 3(a) and 3(b)].

Uniform instability

Looking for the criterion of uniform instability[2] one must take $k_y = 0$ and $\tau \ll 1$. We derive under these conditions, from Eqs. (32)–(34) that the instability will develop when $k_x^2 < 1$. Using the Bean model relation $B = \mu_0 l J_c$, one obtains the criterion for the onset of the uniform flux jump

$$B > B_a = \frac{\pi}{2}\sqrt{\mu_0 C T^*}. \tag{35}$$

This result is independent of the anisotropy.

IV. SPATIAL FLUX PATTERN

When the external magnetic field increases, the wave vector of the instability k_x decreases, while the magnitude of the Re λ increases to zero. This contact point marks the border between the stable and unstable Bean critical state denoted as (k_x^*, k_y^*). The instability can emerge both as spatially uniform $(k_y^* = 0)$ [Fig. 3(a)] and nonuniform, forming a periodical spatial structure along the flux front $(k_y^* \neq 0)$, [Fig. 3(b)] (here $d_y = 2\pi w / k_y^*$ is the dimension period of the structure). The thermal parameter τ determines the type of the emerging unstable structure. In particular, the nonuniform instability appears when $\tau < \tau_c$ [Fig. 3(c)]. The contact point k_x^*, k_y^* is obtained from the equations

$$\mathrm{Re}\,\lambda(k_x^*, k_y^*) = 0; \quad \left(\frac{d\,\mathrm{Re}\,\lambda(k_x, k_y)}{dk_y}\right)_{k_x^*, k_y^*} = 0. \tag{36}$$

From these requirements of λ, one obtains the following conditions for the S function

$$S(k_x^*, k_y^*) = 0, \quad \Delta S(k_x^*, k_y^*) = 0, \tag{37}$$

where $\Delta S(k_x^*, k_y^*)$ represents the discriminant of S

$$S(k_x^*, k_y^*) = \tau q^2 + S_0 q + S_1 = 0, \tag{38}$$

$$\Delta S(k_x^*, k_y^*) = S_0^2 - 4\tau S_1 = 0,$$

$$S_0 = \tau\gamma n a + \frac{1}{\epsilon}\tau a - 1; \quad S_1 = \frac{n\gamma}{\epsilon}\tau a^2 + \gamma a, \tag{39}$$

where $a = k_x^{*2}, q = k_y^{*2}$. The instability occurs at $k_x < k_x^*$. The boundary between uniform and nonuniform instabilities depends on the thermal parameter τ_c, which can be obtained from [Fig. 3(c)] condition

$$\max[\mathrm{Re}\,\lambda(k_x^*, k_y = 0)]_{\tau = \tau_c} = 0, \tag{40}$$

which can also be written as $P(k_x^*, k_y = 0) = 0$ (where $k_x^* > 2\pi w / l$ due to the quasiclassical approximation). Below we consider the appearance of the fingering instability for different relations between the anisotropy parameters.

V. STRONG THERMAL CONDUCTIVITY ANISOTROPY

A. Isotropic voltage-current characteristics: $\gamma = 1$, $(1/\epsilon) \gg n \gg 1$

In this case, the solution to leading order in $n\epsilon \ll 1$ reads

$$k_x^* = \sqrt{\frac{\epsilon}{\tau}}(1 - \sqrt{n\epsilon}); \quad k_y^* \simeq \sqrt[4]{\frac{n\epsilon}{\tau^2}}. \tag{41}$$

The spatially nonuniform instability occurs at $k_x < k_x^*$. One obtains that the nonuniform instability emerges above some critical induction

$$B > B_f = \frac{\pi}{2}\sqrt{\frac{\mu_0^2 T^* \kappa_\parallel J_c}{nE}}. \tag{42}$$

The unstable flux pattern size can be obtained from Eq. (41)

$$d_y = \frac{w}{k_y^*} = \left(\frac{\epsilon}{n}\right)^{1/4}\sqrt{\frac{\kappa_\parallel T^*}{nEJ_c}}. \tag{43}$$

The boundary between uniform and nonuniform instabilities can be obtained from Eq. (40). This equation yields the immediate

$$\tau_c = \sqrt{\frac{\epsilon}{4n}}, \tag{44}$$

and the instability evolves not uniformly for $\tau < \sqrt{\epsilon/4n}$. Rewriting this in dimensional form we conclude that for

$$E > E_c = \sqrt{\frac{\epsilon}{n}} \frac{2\kappa_{\|}\mu_0 J_c}{C}, \tag{45}$$

the unstable pattern appears. Substituting Eq. (45) in Eq. (42) one obtain the critical rate of the external magnetic induction in this case

$$\dot{B}^{\bullet}_{ext} \geq \dot{B}_c \left(\frac{B_{ext}}{B_{fc}}\right)^{-2}, \tag{46}$$

where

$$\dot{B}_c = \frac{\pi^2 \kappa_{\|}\mu_0^2 J_c T^*}{2nlB_{fc}^2}, \quad B_{fc} = (\pi^2 \mu_0 T^* C/4\sqrt{n\varepsilon})^{1/2}, \tag{47}$$

and $B_{ext}=B_f$ (see Fig. 1). Substituting Eq. (45) in Eq. (43) one obtains for the size of the critical pattern in this case

$$d_y = \frac{w}{k_y^*} = d_{yc}\sqrt{\frac{\dot{B}_c}{\dot{B}}}, \tag{48}$$

where $d_{yc}=\sqrt{CT^*/2\mu_0 J_c^2 n}$ is the size of the critical pattern at $\dot{B}=\dot{B}_c$.

B. Extremely anisotropic thermal conductivity: $n\gamma\epsilon \ll 1$

Solving Eqs. (38) and (39) in this limit one obtains

$$k_x^* = \sqrt{\frac{\epsilon}{\tau}}(1-\sqrt{\gamma n \epsilon}); \quad k_y^* = \sqrt{\frac{\sqrt{\gamma n \epsilon}}{\tau}}. \tag{49}$$

Nonuniform instability appears at $k_x < k_x^*$ (see Fig. 4). In this case

$$B_f = \frac{\pi}{2}\sqrt{\frac{\mu_0^2 T^* \kappa_{\|} J_c}{En}}. \tag{50}$$

The unstable flux pattern size can be obtained from Eq. (49)

$$d_y = \frac{w}{k_y^*} = \sqrt[4]{\frac{\epsilon}{\gamma n}}\sqrt{\frac{T^*\kappa_{\|}}{nJ_c E}}. \tag{51}$$

The boundary between uniform and nonuniform instabilities [Eq. (40)] is determined by the condition $\tau < \sqrt{\epsilon/4\gamma n}$, which is valid for the electric field

$$E > E_c = \frac{2\kappa_{\|}\mu_0 J_c}{C}\sqrt{\frac{\gamma\epsilon}{n}}. \tag{52}$$

The unstable pattern arises above the magnetic induction rate $\dot{B}^{\bullet}_{ext} > \dot{B}_c (B_{ext}/B_{fc})^2$ where

$$\dot{B}_c = \frac{\pi^2 \kappa_{\|}\mu_0^2 J_c T^*}{4nlB_{fc}^2}; \quad B_{fc} = \left(\frac{\pi^2}{8}\frac{\mu_0 T^* C}{\sqrt{\gamma\epsilon n}}\right)^{1/2}. \tag{53}$$

while the characteristic size of the critical pattern reads

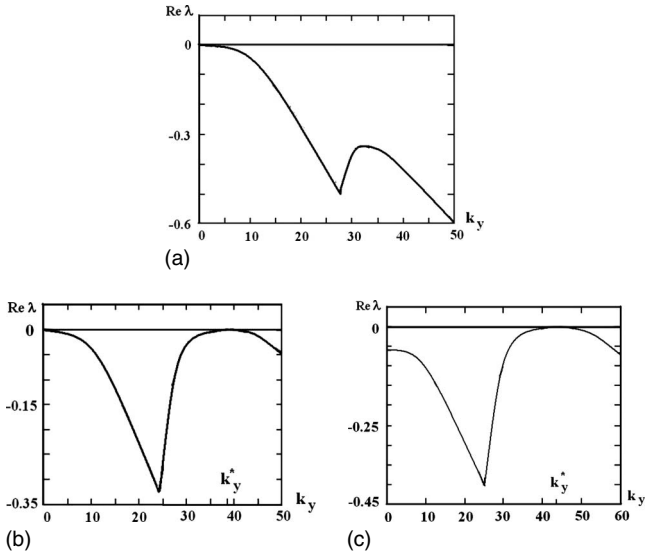

FIG. 4. Contour line Re $\lambda(k_x^*,k_y^*)=0$ for various thermal parameters. τ shows the transition from a uniform to a nonuniform patterned instability at $\tau_c=\sqrt{\epsilon/4\gamma n}$. (a) The single maximum of the Re $\lambda(k_x^*,k_y^*)=0$ at $k_y^*=0$ ($k_x^*=0.301$) demonstrates the uniform instability at $\tau=0.01$. (b) Two equal maxima ($k_y=0, k_y^*=30.5, k_x^*=0.879$) of the Re $\lambda(k_x^*,k_y^*)=0$ show the uniform-to-pattern border curve at $\tau_c=0.00293$. (c) Single maximum of the Re $\lambda(k_x^*,k_y^*)=0$ at $k_y^*=37.5$ ($k_x^*=1.08$) exhibits unstable pattern domain at $\tau=0.00194$. (Here $n=10$, $\gamma=10^2$, and $\epsilon=10^{-4}$).

$$d_{yc} = \sqrt{\frac{CT^*}{\mu_0 n\gamma J_c^2}}. \tag{54}$$

C. Small voltage-current characteristics anisotropy: $n \gg \gamma \gg 1$, $\epsilon \ll 1/n\gamma$

Solving Eqs. (38) and (39) in this limit one obtains

$$k_x^* = \sqrt{\frac{\epsilon}{\tau}}; k_y^* = \sqrt{\frac{\sqrt{n\gamma\epsilon}}{\tau}}. \tag{55}$$

Nonuniform instability appears at $k_x < k_x^*$ when $B > B_f$ (in the Bean approximation)

$$B_f = \frac{\pi}{2}\sqrt{\frac{\mu_0^2 \kappa_{\|} J_c T^*}{nE}}. \tag{56}$$

The unstable flux pattern size can be obtained from Eq. (55)

$$d_y = \frac{w}{k_y^*} = \sqrt[4]{\frac{\epsilon}{\gamma n}}\sqrt{\frac{T^*\kappa_{\|}}{nJ_c E}}. \tag{57}$$

The boundary between uniform and nonuniform instabilities [Eq. (40)] is determined by the condition $\tau < \sqrt{\epsilon/4\gamma n}$, which is valid for the electric field

$$E > E_c = \sqrt{\frac{4\gamma\epsilon}{n}}\frac{\kappa_{\|}\mu_0 J_c}{C}. \tag{58}$$

Both the magnetic induction rate and the size of the critical pattern in this case are similar to those defined by the Eqs. (53) and (54).

D. Equally strong electric and thermal anisotropies: $\gamma \gg n \gg 1$, $\gamma\epsilon=1$

We now discuss the case of systems with strongly anisotropic both voltage-current characteristics and thermal conductivity. In this case Eqs. (38) and (39) give

$$k_x^* = \sqrt{\frac{1}{\gamma n \tau}}; k_y^* = \sqrt{\frac{1}{\tau}\sqrt{\frac{2}{n}}}. \tag{59}$$

The nonuniform instability arises in this case for the same criteria as in the isotropic case, i.e., the same applied magnetic induction $B > B_{fc} = B_{fc}^i$ and the same magnetic induction rate as in the isotropic case.[3] These values were obtained as described above [Eq. (40)] ($k_x > k_x^*$ and $\tau < 1/\gamma n$). The unstable flux pattern also has the same size as in isotropic systems.[3]

VI. SUMMARY

We have concluded that anisotropy of the thermal conductivity in a type-II superconducting slab for a nearly thermally insulating surface assists in the appearance of a nonuniform flux pattern. The effects are better pronounced in systems with strong thermal conductivity while the voltage-current anisotropy is small. The magnetic flux penetrating the anisotropic slab demonstrates features more typical for the instability in superconducting films rather than in isotropic slabs.

The applicability of the present theory is restricted due to both assumption of the homogeneity of the temperature across the sample [see Eq. (12)] and due to the WKB conditions $h_0 \lambda_x < 1, \lambda_x < l$. In particular, the maximal magnitude of the external magnetic-field rate $\dot{B}_m$ can be directly obtained from Eq. (12) demonstrating that, independent of the anisotropy, the experimental magnetic-field rates are bounded from above by the condition ($h_0 l < 1$)

$$\dot{B}_{ext} \leq \dot{B}_{\max} = \frac{4T_0 \kappa_\parallel h_0}{l^2 J_c}. \tag{60}$$

Besides this restriction, several other conditions should be satisfied. First of all, the rate of the magnetic induction $\dot{B}$ change must exceed the critical value $\dot{B}_c$, second, the external magnetic induction $B_{ext} = J_c l \mu_0$ must satisfy the condition $B_{ext} \lesssim B_{fc}$ (see Fig. 1) while the rate of the magnetic induction [see Eq. (46)]

$$B_{ext}^{\bullet} \geq \dot{B}_c \left(\frac{B_{ext}}{B_{fc}} \right)^{-2}. \tag{61}$$

The critical magnetic induction B_{fc}, the magnetic induction rate $\dot{B}_c$, and the characteristic sizes of the critical patterns (domains) d_y are different for various types of anisotropies and are defined by Eqs. (47), (48), (53), and (54). In particular, in the case $\gamma = 1$, $(1/\epsilon) \gg n \gg 1$ [see Eqs. (45)–(48)] one obtains

$$\dot{B}_c / \dot{B}_c^i \simeq 2\sqrt{\frac{\epsilon}{n}}; \quad B_{fc}/B_{fc}^i \simeq (n\epsilon)^{-1/4} \quad d_y/d_i^i \simeq \sqrt{\frac{1}{2n}}, \tag{62}$$

where $\dot{B}_c^i = \mu_0 \kappa_\parallel J_c / Cl; B_{fc}^i = \frac{\pi}{2}\sqrt{T^* \mu_0 C}; d_{yc}^i = (T^* C / \sqrt{2n} \mu_0 J_c^2)^{1/2}$ (Ref. 3) (here $\dot{B}_c^i$, B_{fc}^i, and d_y^i define the rate of magnetic induction, the critical induction at the onset of the instability, and the characteristic size of flux pattern in the isotropic case, respectively).

One can conclude that systems with thermal anisotropy are much more promising for studying pattern instability than isotropic ones. Using a $La_{2-x}Sr_xCuO_4$ superconductor with parameters (see Ref. 17)

$$J_c = 7 \times 10^8 \ \text{A/m}^2, \ l = 10^{-3} \ \text{m}, \ T_0 \simeq 10 \ \text{K},$$
$$T^* \simeq 10 \ \text{K}, \ \epsilon = 10^{-3},$$
$$n = 30, \ C = 10^4 \ \text{J/Km}^3, \ k_\parallel = 5 \times 10^{-1} \ \text{W/Km},$$
$$h_0 = 2 \times 10^2 \ \text{m}, \tag{63}$$

one obtains in this case

$$B_{ext} = 0.7 \ \text{T}, \ B_{fc} \simeq 1.2 \ \text{T}, \ \dot{B}_{\max} \simeq 6 \ \text{T/sec},$$
$$\dot{B}_c \simeq 0.4 \ \text{T/sec}, \ d_y \simeq 0.02 \ \mu\text{m}.$$

The instability arises [see Eq. (61)] above $B_{ext}^{\bullet} \simeq 0.6$ T/sec.

ACKNOWLEDGMENTS

We appreciate the useful discussion with Yu. Galperin, Y. Yeshurun and A. Shaulov and acknowledge support from the Israel Scientific Foundation (Grant No. 499/07).

[1] D. V. Denisov, A. L. Rakhmanov, D. V. Shantsev, Y. M. Galperin, and T. H. Johansen, Phys. Rev. B **73**, 014512 (2006).
[2] R. G. Mints and A. L. Rakhmanov, Rev. Mod. Phys. **53**, 551 (1981).
[3] A. L. Rakhmanov, D. V. Shantsev, Y. M. Galperin, and T. H. Johansen, Phys. Rev. B **70**, 224502 (2004).
[4] V. K. Vlasko-Vlasov, V. I. Nikitenkoa, A. A. Polyanskiia, G. W. Crabtreeb, U. Welp, and B. W. Veal, Physica C **222**, 361 (1994).
[5] M. R. Koblischka, T. H. Johansen, M. Baziljevich, H. Hauglin, H. Bratsberg, and B. Ya. Shapiro, Europhys. Lett. **41**, 419 (1998).
[6] D. Barness, M. Sinvani, A. Shaulov, T. Tamegai, and Y. Yeshurun, Phys. Rev. B **77**, 094514 (2008).
[7] C. A. Duran, P. L. Gammel, R. E. Miller, and D. J. Bishop, Phys. Rev. B **52**, 75 (1995).
[8] I. S. Aranson, A. Gurevich, and V. M. Vinokur, Phys. Rev. Lett. **87**, 067003 (2001).
[9] F. Bass, B. Ya. Shapiro, I. Shapiro, and M. Shvartser, Phys. Rev.

B **58**, 2878 (1998).
[10] I. S. Aranson, A. Gurevich, M. S. Welling, R. J. Wijngaarden, V. K. Vlasko-Vlasov, V. M. Vinokur, and U. Welp, Phys. Rev. Lett. **94**, 037002 (2005).
[11] E. Deutsch, B. Ya. Shapiro, and I. Shapiro, Physica C **468**, 23 (2008).
[12] L. M. Fisher, P. E. Goa, M. Baziljevich, T. H. Johansen, A. L. Rakhmanov, and V. A. Yampol'skii, Phys. Rev. Lett. **87**, 247005 (2001).
[13] M. F. Crommie and A. Zettl, Phys. Rev. B **43**, 408 (1991); V. B. Efimov and L. P. Mezhov-Deglin, Fiz. Nizk. Temp. **23**, 278 (1997); Low Temp. Phys. **23**, 204 (1997).
[14] A. V. Gurevich, Phys. Rev. Lett. **65**, 3197 (1990).
[15] E. E. Dvash, I. Shapiro, and B. Ya. Shapiro, Europhys. Lett. **83**, 67005 (2008).
[16] E. M. Lifshitz and L. P. Pitaevskii, *Course of Theoretical Physics: Physical Kinetics*, Course of Theoretical Physics Series: Vol. 10 (Pergamon, New York, 1981).
[17] D. M. Ginzberg, *Physical Properties of High Temperature Superconductors III* (World Scientific, Singapore, 1992).